

Fractal Conductance Fluctuations in Gold–Nanowires

Helmut Hegger¹, Bodo Huckestein², Klaus Hecker¹, Martin Janssen², Axel Freimuth³, Gernot Reckziegel¹,
Rüdiger Tuzinski⁴

¹ *II. Physikalisches Institut, Universität zu Köln, D-50937 Köln, Germany*

² *Institut für Theoretische Physik, Universität zu Köln, D-50937 Köln, Germany*

³ *Physikalisches Institut, Universität Karlsruhe, D-76128 Karlsruhe, Germany*

⁴ *Institut für Halbleitertechnik der Technischen Hochschule Aachen, D-52056 Aachen, Germany*

(December 7, 2017)

A detailed analysis of magnetoconductance fluctuations of quasiballistic gold-nanowires of various lengths is presented. We find that the variance $\langle(\Delta G)^2\rangle = \langle(G(B) - G(B + \Delta B))^2\rangle$ when analyzed for ΔB much smaller than the correlation field B_c varies according to $\langle(\Delta G)^2\rangle \propto \Delta B^\gamma$ with $\gamma < 2$ indicating that the graph of G vs. B is fractal. We attribute this behavior to the existence of long-lived states arising from chaotic trajectories trapped close to regular classical orbits. We find that γ decreases with increasing length of the wires.

PACS numbers: 73.23.-b, 73.50.Jt

It is well established that quantum interference modifies the conductance G of disordered conductors and ballistic devices smaller than the phase coherence length L_φ (mesoscopic regime) [1]. In a semiclassical description one may view the conductance electrons as moving along their classical trajectories, i.e. ballistically between collisions. Since the phase information is not lost over distances of order L_φ , a sample specific interference pattern arises. This interference pattern may be altered e.g. by applying a magnetic field B , which gives rise to reproducible conductance fluctuations (CF) [1–7].

It has recently been pointed out by Ketzmerick [8] that the dwell time probability $P(t)$ for an electron to stay in the mesoscopic sample longer than a time t is related intimately to the statistical properties of the CF. It is often assumed that the typical time to cross the system, t_D , determines the behavior of $P(t)$ for times larger than t_D ,

$$P(t) \propto e^{-t/t_D}. \quad (1)$$

This form gives rise to a Lorentzian shape of the energy-dependent conductance autocorrelation function $C(\Delta E) = \langle\delta G(E)\delta G(E + \Delta E)\rangle$ with $\delta G(E) = G(E) - \langle G(E)\rangle$ and correlation energy $E_c = \hbar/t_D$ [3,9–11]. Since $C(\Delta E) = C(0) - 0.5\langle(\Delta G)^2\rangle$ the variance $\langle(\Delta G)^2\rangle = \langle(G(E) - G(E + \Delta E))^2\rangle$ behaves as $\langle(\Delta G)^2\rangle \propto \Delta E^2$ for $\Delta E \ll E_c$.

The validity of Eq. (1) has been questioned by several authors [8,12,13,20] and long-lived states have been predicted. If $P(t)$ does not vary exponentially but decays algebraically,

$$P(t) \propto t^{-\gamma}, \quad 0 < \gamma \leq 2 \quad (2)$$

a non-trivial behavior of the variance appears [8]:

$$\langle(\Delta G)^2\rangle \propto \Delta E^\gamma \quad \text{for } \Delta E \ll E_c. \quad (3)$$

It is important to note that exponents γ in Eq. (2) which are larger than two cannot be detected in the variance.

For $\gamma > 2$ the variance stays quadratic with respect to ΔE since analytic behavior dominates the lowest order approximation.

Measuring the length of the graph G vs. E on a scale ΔE leads, as a consequence of Eq. (3), to a divergence proportional to $(\Delta E)^{-(1-\gamma/2)}$, i.e. the graph is fractal with fractal dimension $D_F = 2 - \gamma/2$ [15].

The conclusions discussed here for time t and energy E hold similarly for other pairs of canonically conjugate variables, e.g. for “area” A and magnetic field B , since for a closed path A can be considered as the accumulated area of an electron moving along the path in time t .

In this letter we present measurements of the magnetoconductance fluctuations of weakly disordered quasiballistic gold-nanowires with various lengths $L < L_\varphi$. We adopt the method suggested by Ketzmerick [8]. The analysis of $G(B)$ yields that $\langle(\Delta G)^2\rangle \propto \Delta B^\gamma$, where γ is significantly smaller than two and decreases with increasing length of the nanowire. We attribute this behavior to the existence of long-lived states in the mesoscopic wire with a dwell time probability $P(t)$ decaying much slower than exponentially. In addition we find that the graph G vs. B is indeed fractal with fractal dimension $D_F = 2 - \gamma/2$.

Gold-nanowires of very high purity (99.999%) were fabricated using electron-beam lithography and lift-off with a four layer polymethylmethacrylate- (PMMA) based resist system as described in Ref. [16]. The wires had a cross-section of 30×30 nm² and lengths between 400 nm and 1000 nm with a resolution of ± 5 nm. Current- and voltage-probes were connected to the wires as shown in the inset of Fig. 4, providing a mesoscopic 2-probe arrangement [6]. The conductance $G(B)$ was measured as a function of the magnetic field B ($|B| \leq 6$ T, 1 mT step-size) with a standard ac lock-in technique in a ³He–⁴He-dilution refrigerator at $T \approx 60$ mK [6].

The total resistance (nanowire and contacts) at $T = 60$ mK varies between $R = 8.2 \Omega$ and $R = 18.3 \Omega$ for $L = 400$ nm and $L = 1000$ nm, respectively. The re-

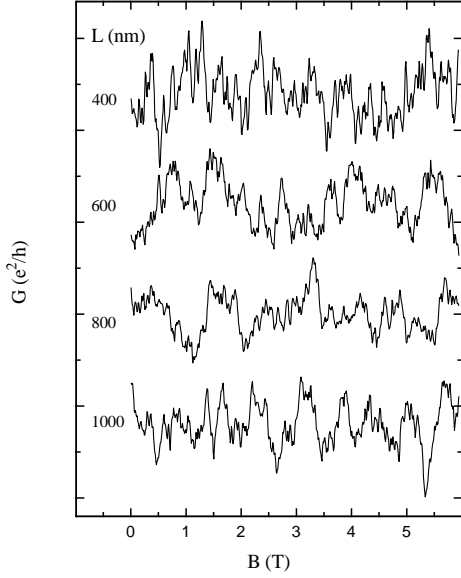


FIG. 1. Conductance $G(B)$ as a function of the magnetic field B for 4 Au-wires with lengths as given in the figure. The traces are shifted along the y-axis for clarity. (See text.)

sistance R_c of the two funnel-shaped contacts is 2.4Ω , as calculated from the resistance per square $R_{\square} = 0.5 \Omega$. From the residual resistance ratio $R_{77K}/R_{4.2K}$ and from the electron phonon inelastic scattering rate we obtain an elastic mean free path ℓ in all investigated devices of $\ell \approx 60$ nm. This is larger than the width $W \simeq 30$ nm and the thickness $T = 30$ nm of the wires and much larger than the Fermi-wavelength in gold ($\lambda_F \simeq 0.52$ nm), i.e. our wires are in the quasiballistic limit. The phase-coherence length as determined from weak localization at $T = 100$ mK is $L_{\varphi} \approx 1.3 \mu\text{m}$; the spin-orbit scattering length is $L_{s.o.} \approx 0.2 \mu\text{m}$ [17].

In Fig. 1 we show $G(B) = G^{exp}(B) - G^{cl}(B)$ for four samples of different lengths. Here $G^{exp}(B)$ is the conductance as measured at 60 mK. $G^{cl} \propto B^2$ is the weak classical magnetoconductance obtained from a quadratic fit to $G^{exp}(B)$. The rms-amplitude of the CF is of order $\text{rms}(G) \approx 0.11 e^2/h$ for all wires.

The correlation field B_c as determined from the half-width of the autocorrelation function $C(\Delta B) = \langle G(B)G(B + \Delta B) \rangle$ ranges between 37 mT and 85 mT (see Tab. 1). The weak dependence of B_c on L is related to the non-locality of the CF and was discussed elsewhere [6].

Before we analyze $\langle (\Delta G)^2 \rangle$ we estimate the contribution of the experimental noise to the measured conductance as compared to that of the reproducible CF. We write the total conductance as $G(B) = G_{cf}(B) + G_n(B)$, where G_{cf} denotes the reproducible part and G_n is due to noise. Since $G(B)$ is measured in a mesoscopic 2-probe configuration the CF are symmetric with respect to reversal of the magnetic field, i.e. $G_{cf}(B) = G_{cf}(-B)$.

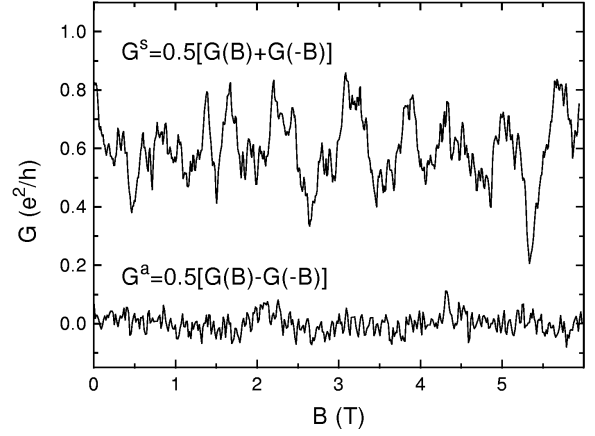


FIG. 2. Symmetric G^s and antisymmetric part G^a of $G(B)$. G^a is a measure of noise, whereas G^s measures the reproducible conductance fluctuations (see text). G^s is shifted by $0.6 e^2/h$ for clarity.

On the other hand, the noise component of a particular magnetoconductance trace may be viewed as being composed of symmetric and antisymmetric parts G_n^s and G_n^a , where $G_n^s \equiv [G_n(B) + G_n(-B)]/2$, and $G_n^a \equiv [G_n(B) - G_n(-B)]/2$, so that $G_n^a(B) + G_n^s(B) = G_n(B)$, $G_n^s(B) = G_n^s(-B)$, and $G_n^a(B) = -G_n^a(-B)$. The antisymmetric part of the total conductance $G^a = [G(B) - G(-B)]/2$ is a measure of the antisymmetric noise component $G^a = G_n^a$. The symmetric part $G^s = [G(B) + G(-B)]/2$ is given by $G^s = G_{cf} + G_n^s$. Since it is reasonable to assume that the symmetric and antisymmetric experimental noise components are of equal magnitude the noise contribution to G^s (and thus to G) can be estimated from G^a .

As an example we show in Fig. 2 G^a and G^s for the 1000 nm long wire. Similar results are obtained for all other wires. The rms-noise-amplitude $\text{rms}(G_n^a) \approx \text{rms}(G_n^s)$, calculated in the magnetic field range up to 6 T, is of order $\text{rms}(G_n^{s,a}) \leq 0.03 e^2/h$ which is clearly smaller than the amplitude of the reproducible CF amplitude $\text{rms}(G) \approx 0.11 e^2/h$ (see Tab. 1). It should be noted that the rms-noise-amplitudes $\text{rms}(G_n^a)$ calculated on magnetic field scales $\Delta B < B_c$, which are relevant for the determination of γ , are much smaller ($\leq 0.007 e^2/h$). This is a reflection of the $1/f$ -component of the total experimental noise as function of the magnetic field [14]. The value for the rms-noise-amplitude obtained from G^a is in accordance with a more direct method where we measured the system noise at a fixed magnetic field ($B = 0$ T).

We turn now to the calculation of $\langle (\Delta G)^2 \rangle$ as a function of ΔB . We have used both, $G(B)$ and $G^s(B)$ for this calculation. Figure 3 shows on a double logarithmic scale $\langle (\Delta G)^2 \rangle$ as a function of ΔB . We also analyzed the experimental noise $\langle (\Delta G^a)^2 \rangle$ (inset of Fig. 3). As shown, the values of the derivative $d \ln \langle (\Delta G)^2 \rangle / d \ln(\Delta B)$ for the

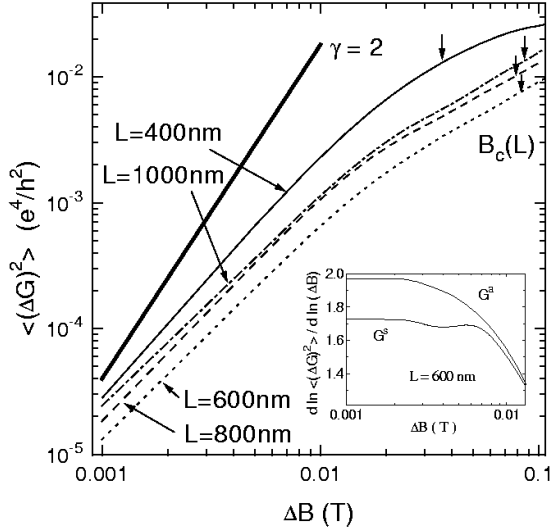


FIG. 3. Variance $\langle(\Delta G)^2\rangle$ calculated from $G^s(B)$ as a function of ΔB for the gold-wires on a double logarithmic scale. The correlation fields B_c are indicated by the arrows. The slope γ of $\langle(\Delta G)^2\rangle$ versus ΔB has been extracted by linear fits in the region $2 - 3 \text{ mT} \leq \Delta B \leq 10 \text{ mT} \ll B_c$. For comparison we show a thick solid line of slope 2. Inset: logarithmic derivative $d \ln \langle(\Delta G^{s,a})^2\rangle / d \ln(\Delta B)$ for the nanowire with $L = 600 \text{ nm}$.

noise G^a are higher than those for G^s . A region, approximately flat, which corresponds to a power law behavior with $\gamma < 2$ can only be observed for G^s . Therefore, it is clear that the observation of $\gamma < 2$ for G^s is not caused by experimental noise.

We find that $\langle(\Delta G)^2\rangle$ varies as ΔB^γ for $\Delta B \ll B_c$ with an uncertainty of the exponent of ± 0.05 (see Tab. 1). Thus we conclude that at least for the wires of length $L \geq 600 \text{ nm}$ γ is definitely smaller than 2 which indicates long-lived states with a dwell time probability $P(t) \propto t^{-\gamma}$. In addition we find that γ decreases with increasing system length L of the nanowires (see Fig. 4) while the signal to noise ratio increases. We also performed a direct fractal analysis on the graph G vs. B [15]. The results obtained are in very good agreement with those analyzing the variance and are listed in table 1. Measurements at higher temperatures ($T \leq 4.2 \text{ K}$) or on longer wires with ratio $L/L_\varphi \lesssim 2$ show reduced CF and no significant change in the exponent γ .

For comparison we have also measured various disordered aluminum nanowires with $\lambda_F \approx \ell \ll W, T$ and phase coherence length $L_\varphi \approx 350 \text{ nm} < L = 500, 1000, 1500 \text{ nm}$. All the wires show values of $\gamma = 2$ within the experimental uncertainty.

Now we turn to the discussion of our results. As outlined in the introduction the observation of $\gamma < 2$ indicates the existence of long-lived states. We know of two possible explanations for the existence of long-lived

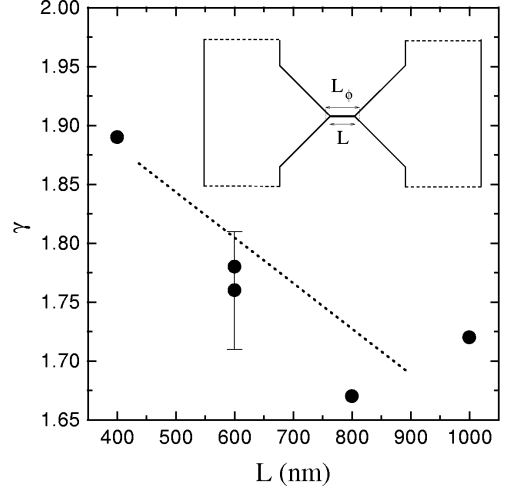


FIG. 4. γ versus L (see text). The inset shows the sample layout, i.e. a Au-nanowire of length $L = 1\mu\text{m}$ with two funnel-shaped current-voltage probes with an opening angle of 90° . This corresponds to a mesoscopic 2-probe arrangement; current- and voltage-leads are attached far outside the phase-coherence volume. The dotted line serves as guide to the eye.

states in mesoscopic conductors. To distinguish between them it is helpful to consider the classification of mesoscopic conductors as introduced recently by Aleiner and Larkin [18]. A mesoscopic conductor for which the electronic path between scattering events can be considered as purely classical was denoted as being in the quantum chaos (QC) regime. In this case, not only the Fermi wavelength λ_F has to be much smaller than the (transport) mean free path ℓ but also the typical scale d over which the potential energy varies has to satisfy the constraint $d^2 > \lambda_F \ell$. Typical examples for such systems are antidot arrays [19] where d plays the role of the diameter of an antidot and ballistic cavities where d coincides with the size of a cavity. Conductors with $d^2 < \lambda_F \ell$ are denoted as being in the quantum disorder (QD) regime since the uncertainty δx of the electron position in the direction of its momentum after a collision is larger than d .

It is now well known [8] that in the QC regime the corresponding classical phase space is neither fully chaotic nor fully integrable but contains in general islands of regular trajectories with a self-similar structure. Those classical chaotic trajectories that spend long time close to regular orbits give rise to power law behavior in the classical dwell time probability $P(t) \propto t^{-\gamma}$. So far the prediction of the exponent γ for a given system does not seem to be possible. However, according to Ketzmerick [8] several values for γ which are of $\mathcal{O}(1)$ have been reported for ballistic cavities as well as for antidot arrays.

Another approach to the existence of long-lived states goes back to the work of Altshuler et.al.(AKL) [12]. They claim that quasi-localized states already exist in

L (μm)	G (e^2/h)	rms(G) (e^2/h)	B_c (mT)	γ^*	γ	γ_F
0.4	3135	0.105	37	1.86	1.89	1.88
0.6a	1968	0.13	80	1.77	1.78	1.75
0.6b	1645	0.12	80	1.68	1.76	1.74
0.8	1286	0.1	78	1.75	1.68	1.68
1.0	1408	0.1	85	1.74	1.72	1.70

TABLE I. L : Length of the nanowires; G : Total conductance; rms(G): Root-mean-square of the CF with an accuracy of $\pm 0.01 e^2/h$; B_c : Correlation field extracted from the half-width of the autocorrelation function $C(\Delta B)$ with an accuracy of ± 10 mT; γ^* and γ have been extracted by fits of the variance $\langle(\Delta G)^2\rangle$ calculated from $G(B)$ and $G^s(B)$, respectively with an uncertainty of ± 0.05 . γ_F was obtained by a direct fractal analysis of the graph G vs. B with an uncertainty of ± 0.04 .

the metallic regime of mesoscopic conductors with a non-exponentially small probability. These states are trapped by Bragg reflection in an optimal potential fluctuation and should appear in the QC as well as in the QD regimes. They have attracted considerable interest in the last two years and the results of AKL have been confirmed and improved [13,20]. The crucial result is that due to such quasi-localized states the dwell time probability (in a wire) should behave for not to large times $t \gg t_D$ as:

$$P(t) \propto \exp(-g \ln^2(t/t_D)) \propto t^{-g \ln(t/t_D)}. \quad (4)$$

Here $g = Gh/e^2$ is the dimensionless conductance which is large in a metallic wire, $g \gg 1$ (see Tab. 1). Thus one cannot detect the corresponding long-lived states in the CF which are only sensitive to a power law behavior in $P(t)$ with an exponent γ smaller than two.

Turning now to our experiments we note that our gold-wires are characterized by an elastic mean free path which is caused mainly by diffusive boundary scattering, $\ell > W, T$. In addition there is also a certain amount of specular boundary scattering and one may classify the samples as QC conductors with $d \approx W$. We therefore conclude that the observed behavior of the variance $\langle(\Delta G)^2\rangle \propto \Delta B^\gamma$ in the Au-wires indicates the existence of long-lived states with a dwell time probability $P(t) \propto t^{-\gamma}$, $\gamma < 2$. In contrast, the aluminum wires are definitely in the QD regime, since $\lambda_F \approx \ell$, consistent with $\gamma \simeq 2$.

In summary, we have presented measurements of magnetoconductance fluctuations in mesoscopic gold-wires, which are in the quantum chaos regime. Analysis of the CF-pattern reveals power law behavior of the variance $\langle(\Delta G)^2\rangle = \langle(G(B) - G(B + \Delta B))^2\rangle \propto \Delta B^\gamma$ with $\gamma < 2$ for small magnetic field intervals $\Delta B \ll B_c$. This non-analyticity of $\langle(\Delta G)^2\rangle$ is a signature of long-lived states in the samples. Such states are a generic feature of systems with a mixed (chaotic and regular) phase space of the corresponding classical system. Additional measure-

ments, e.g. of the temperature dependence of γ , should provide further insight into the origin of the fractal conductance fluctuations.

We thank R. Schäfer, B. Büchner, R. Ketzmerick, J. Hajdu and H. Micklitz for useful discussions. This work was supported by the Deutsche Forschungsgemeinschaft through SFB 341.

-
- [1] S. Washburn and R. A. Webb, Rep. Prog. Phys. **55**, 1311 (1992), and references therein.
 - [2] P. A. Lee and A. D. Stone, Phys. Rev. Lett. **55**, 1662 (1985); B. L. Altshuler, JETP Lett. **41**, 648 (1985); P. A. Lee, A. D. Stone, and H. Fukuyama, Phys. Rev. B **35**, 1039 (1987).
 - [3] C. M. Marcus, A. J. Rimberg, R. M. Westervelt, P. F. Hopkins, and A. C. Gossard, Phys. Rev. Lett. **69**, 506 (1992).
 - [4] C. M. Marcus, R. M. Westervelt, P. F. Hopkins, and A. C. Gossard, Phys. Rev. B **48**, 2460 (1993).
 - [5] A. M. Chang, H. U. Baranger, L. N. Pfeifer, and K. W. West, Phys. Rev. Lett. **73**, 2111 (1994).
 - [6] K. Hecker, H. Hegger, R. Schäfer, U. Murek, C. Braden, and W. Langheinrich, Phys. Rev. B **50**, 18601 (1994).
 - [7] E. Scheer, H. v. Löhneysen, and H. Hein, Physica B **218**, 85 (1996).
 - [8] R. Ketzmerick, preprint cond-mat/9510007 (1995), accepted for publication in Phys. Rev. B, Oct. 15 (1996), and references therein.
 - [9] R. A. Jalabert, H. U. Baranger, and A. D. Stone, Phys. Rev. Lett. **65**, 2442 (1990); H. U. Baranger, D. P. DiVincenzo, Phys. Rev. B, 10637 (1991); H. U. Baranger, R. A. Jalabert, and A. D. Stone, Phys. Rev. Lett. **70**, 3876 (1993).
 - [10] M. J. Berry, J. A. Katine, R. M. Westervelt, and A. C. Gossard, Phys. Rev. B **50**, 17721 (1994).
 - [11] M. V. Budantsev, Z. D. Kvon, A. G. Pogosov, L. V. Litvin, V. G. Mansurov, V. P. Migal, S. P. Moshchenko, and Yu. Nastaushev, JETP Lett. **59**, 645 (1994).
 - [12] B. L. Altshuler, V. E. Kravtsov, and I. V. Lerner, JETP Lett. **45**, 199 (1987); in *Mesoscopic Phenomena in Solids*, edited by B. L. Altshuler, P. A. Lee, and R. A. Webb (North-Holland, Amsterdam, 1991), p. 449.
 - [13] B. A. Muzykantskii and D. E. Khmelnitskii, Phys. Rev. B **51**, 5480 (1995); B. A. Muzykantskii and D. E. Khmelnitskii, preprint cond-mat/9601045 (1996), (unpublished).
 - [14] The fourier transform of $G^a(B)$ shows a 1/f-noise component for frequencies corresponding to magnetic field changes $\Delta B \geq 12\text{mT}$.
 - [15] B. B. Mandelbrot, *The Fractal Geometry of Nature* (Freeman, San Francisco, 1982).
 - [16] W. Langheinrich, H. Beneking, U. Murek, C. Braden, and D. Wohlleben, J. Vac. Sci. Technol. B **9**, 2904 (1991).
 - [17] U. Murek, thesis, University of Cologne (1991), (unpublished).
 - [18] I. L. Aleiner and A. I. Larkin, preprint cond-mat/9603121

(1996), (unpublished).

- [19] D. Weiss, M. L. Roukes, A. Menschig, P. Grambow, K. von Klitzing, and G. Weimann, Phys. Rev. Lett **66**, 2790 (1991).
- [20] A. D. Mirlin, JETP Lett. **62**, 603 (1995).